


LI

LABORATORY INVESTIGATION

THE BASIC AND TRANSLATIONAL PATHOLOGY RESEARCH JOURNAL

ABSTRACTS

ENDOCRINE PATHOLOGY (296-310)



USCAP 110TH ANNUAL MEETING
**NEVER STOP
LEARNING**
2021

MARCH 13-18, 2021

VIRTUAL AND INTERACTIVE

Published by
SPRINGER NATURE
www.ModernPathology.org

 **USCAP** AN OFFICIAL JOURNAL OF THE
UNITED STATES AND CANADIAN
ACADEMY OF PATHOLOGY
Creating a Better Pathologist

EDUCATION COMMITTEE

Jason L. Hornick
Chair

Rhonda K. Yantiss, Chair
Abstract Review Board and Assignment Committee

Kristin C. Jensen
10 Chair, CME Subcommittee

Laura C. Collins
Interactive Microscopy Subcommittee

Raja R. Seethala
Short Course Coordinator

Ilan Weinreb
Subcommittee for Unique Live Course Offerings

David B. Kaminsky
(Ex-Officio)
Zubair W. Baloch
Daniel J. Brat
Sarah M. Dry
William C. Faquin
Yuri Fedoriw
Karen Fritchie
Jennifer B. Gordetsky
Melinda Lerwill
Anna Marie Mulligan

Liron Pantanowitz
David Papke,
Pathologist-in-Training
Carlos Parra-Herran
Rajiv M. Patel
Deepa T. Patil
Charles Matthew Quick
Lynette M. Sholl
Olga K. Weinberg
Maria Westerhoff
Nicholas A. Zoumberos,
Pathologist-in-Training

ABSTRACT REVIEW BOARD

Benjamin Adam
Rouba Ali-Fehmi
Daniela Allende
Ghassan Allo
Isabel Alvarado-Cabrero
Catalina Amador
Tatjana Antic
Roberto Barrios
Rohit Bhargava
Luiz Blanco
Jennifer Boland
Alain Borczuk
Elena Brachtel
Marilyn Bui
Eric Burks
Shelley Caltharp
Wenqing (Wendy) Cao
Barbara Centeno
Joanna Chan
Jennifer Chapman
Yunn-Yi Chen
Hui Chen
Wei Chen
Sarah Chiang
Nicole Cipriani
Beth Clark
Alejandro Contreras
Claudiu Cotta
Jennifer Cotter
Sonika Dahiya
Farbod Darvishian
Jessica Davis
Heather Dawson
Elizabeth Demicco
Katie Dennis
Anand Dighe
Suzanne Dintzis
Michelle Downes

Charles Eberhart
Andrew Evans
Julie Fanburg-Smith
Michael Feely
Dennis Firchau
Gregory Fishbein
Andrew Folpe
Larissa Furtado
Billie Fyfe-Kirschner
Giovanna Giannico
Christopher Giffith
Anthony Gill
Paula Ginter
Tamar Giorgadze
Purva Gopal
Abha Goyal
Rondell Graham
Alejandro Gru
Nilesh Gupta
Mamta Gupta
Gillian Hale
Suntrea Hammer
Malini Harigopal
Douglas Hartman
Kammi Henriksen
John Higgins
Mai Hoang
Aaron Huber
Doina Ivan
Wei Jiang
Vickie Jo
Dan Jones
Kirk Jones
Neerja Kambham
Dipti Karamchandani
Nora Katabi
Darcy Kerr
Francesca Khani

Joseph Khoury
Rebecca King
Veronica Klepeis
Christian Kunder
Steven Lagana
Keith Lai
Michael Lee
Cheng-Han Lee
Madelyn Lew
Faqian Li
Ying Li
Haiyan Liu
Xiuli Liu
Lesley Lomo
Tamara Lotan
Sebastian Lucas
Anthony Magliocco
Kruti Maniar
Brock Martin
Emily Mason
David McClintock
Anne Mills
Richard Mitchell
Neda Moatamed
Sara Monaco
Atis Muehlenbachs
Bitu Naini
Dianna Ng
Tony Ng
Michiya Nishino
Scott Owens
Jacqueline Parai
Avani Pendse
Peter Pytel
Stephen Raab
Stanley Radio
Emad Rakha
Robyn Reed

Michelle Reid
Natasha Rekhman
Jordan Reynolds
Andres Roma
Lisa Rooper
Avi Rosenberg
Esther (Diana) Rossi
Souzan Sanati
Gabriel Sica
Alexa Siddon
Deepika Sirohi
Kalliopi Siziopikou
Maxwell Smith
Adrian Suarez
Sara Szabo
Julie Teruya-Feldstein
Khin Thway
Rashmi Tondon
Jose Torrealba
Gary Tozbikian
Andrew Turk
Evi Vakiani
Christopher VandenBussche
Paul VanderLaan
Hannah Wen
Sara Wobker
Kristy Wolniak
Shaofeng Yan
Huihui Ye
Yunshin Yeh
Anjana Yeldandi
Gloria Young
Lei Zhao
Minghao Zhong
Yaolin Zhou
Hongfa Zhu

To cite abstracts in this publication, please use the following format: **Author A, Author B, Author C, et al. Abstract title (abs#). In "File Title." *Laboratory Investigation* 2021; 101 (suppl 1): page#**

296 Hypomethylation of SLC5A5 and SLC5A8 5'-Regulatory Regions (5'-RRs) in Poorly Differentiated Thyroid Carcinomas (PDTC)

Juan de Dios Bolaños¹, Teutli Zuno-Coronado², Beatriz Sánchez-Hernández¹, Armando Gamboa-Dominguez¹

¹Instituto Nacional de Ciencias Médicas y Nutrición Salvador Zubirán, Mexico City, Mexico, ²Centro Medico Naval, Ciudad de México, Mexico

Disclosures: Juan de Dios Bolaños: None; Teutli Zuno-Coronado: None; Beatriz Sánchez-Hernández: None; Armando Gamboa-Dominguez: None

Background: Epigenetic modifications in iodine transporters are suspected in radioactive iodine-refractory (RAIR) thyroid carcinomas. PDTC contributes more than half RAIR carcinomas with low survival.

Design: A retrospective search of tumors fulfilling Turin/MSKCC criteria of PDTC (1997-2019), was performed, and compared with rPTC submitted to thyroidectomy + lymphadenectomy + radioactive iodine ablation, half of them RAIR. Clinical data, treatment and follow-up were obtained from electronic records. Macro dissection of tumours, extraction and bisulfite conversion/purification of 800ng DNA were performed. Amplification and pyrosequencing of both 5'-RRs (SLC5A5 Chr 19:17870272-17870308; SLC5A8 Chr 12: 12:101209671-101209705) were carried out with pre-designed PCR and sequencing primers specific for CpG regions (Pyromark assays, Qiagen). Survival curves and non-parametric tests were used.

Results: Among 1,281 malignant tumors, 17(1.3%) were PDTC and were compared with 16 rPTC. PDTC were observed in older patients (68 vs 47 y-o; p=0.001), showed more frequent distant metastases (73 vs 31%; p=0.03), had shorter survival (104 vs 204 months; p=0.02. Graphic) and larger size (7.3 vs 3.1 cm; p<0.001) compared to rPTC. 11(64.7%) met Turin, 12(70.5%) MSKCC and 6(35.2%) both criteria (Figure). PDTC methylation level was lower in SLC5A5 and SLC5A8 as compared with rPTC (21.3/7.6% vs. 42.8/15.8%, respectively; p <0.001) and remnant thyroid tissue (21.3/7.6% vs. 40/10.9%, respectively; p <0.001). rPTC and RAIR rPTC had similar methylation in both regions.

	Recurrent papillary thyroid carcinomas	Poorly differentiated thyroid carcinomas	Normal thyroid tissue	p
Age (Mean ± SD)	46.75 (± 15.23)	68.29 (± 13.45)		.001
Sex (F:M)	4.3:1	3.2:1		.537
Follow up in months (Mean ± SD)	129 (± 40.2)	49.2 (± 42.7)		<.001
Cumulative dose of radioactive iodine (Mean ± SD)	478.3 (± 78.4)	364.2 (± 211.6)		.252
AJCC 8 Stage (n, %)				.097
Stage I + II	11 (84.6)	6 (46.2)		
Stage III + IV	2 (15.4)	7 (53.8)		
Tumor size (Mean ± SD)	3.14 (± 1.8)	7.3 (± 4.5)		<.001
Focality (n, %)				.273
Unifocal	5 (38.4)	6 (60)		
Multifocal	8 (61.5)	4 (40)		
Cervical lymph node metastasis rate (mean % ± SD)	54.5 (± 30.4)	31 (± 32)		.082
Lymph nodes dissected (Mean ± SD)	15.7 (± 11.2)	10.5 (± 13.36)		.093
Distant metastasis (n, %)				.032
Present	5 (31.3)	11 (73.3)		
Absent	11 (68.8)	4 (26.7)		
Margins (n, %)				.375
Positive	6 (54.5)	9 (69.2)		
Negative	5 (45.5)	4 (30.8)		
%meth_CpG1a6_5a5 (Mean ± SD)	42.8 (23.7)	21.3 (10.8)	40.0 (8.7)	<.001
%meth_CpG1a5_5a8 (Mean ± SD)	15.8 (8.5)	7.6 (3.3)	10.9 (2.6)	<.001
Turin criteria (n, %)		11 (64.7%)		
MSKCC criteria (n, %)		12 (70.5%)		
Turin and MSKCC criteria (n, %)		6 (35.2%)		

Abbreviations: AJCC 8, American Joint Committee on Cancer 8; MSKCC, Memorial Sloan Kettering Center

Figure 1 - 296

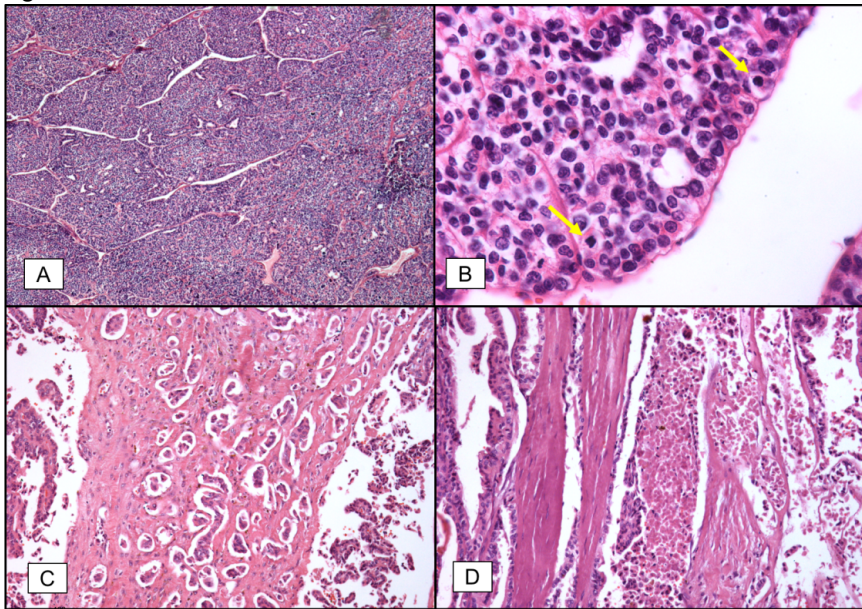


Figure 1. (A,B) PDTC based on Turin criteria with solid and insular growth patterns showing numerous mitosis (yellow arrows). (C,D) PDTC based on MSKCC criteria showing papillary and micropapillary growth patterns with necrosis.

Figure 2 - 296

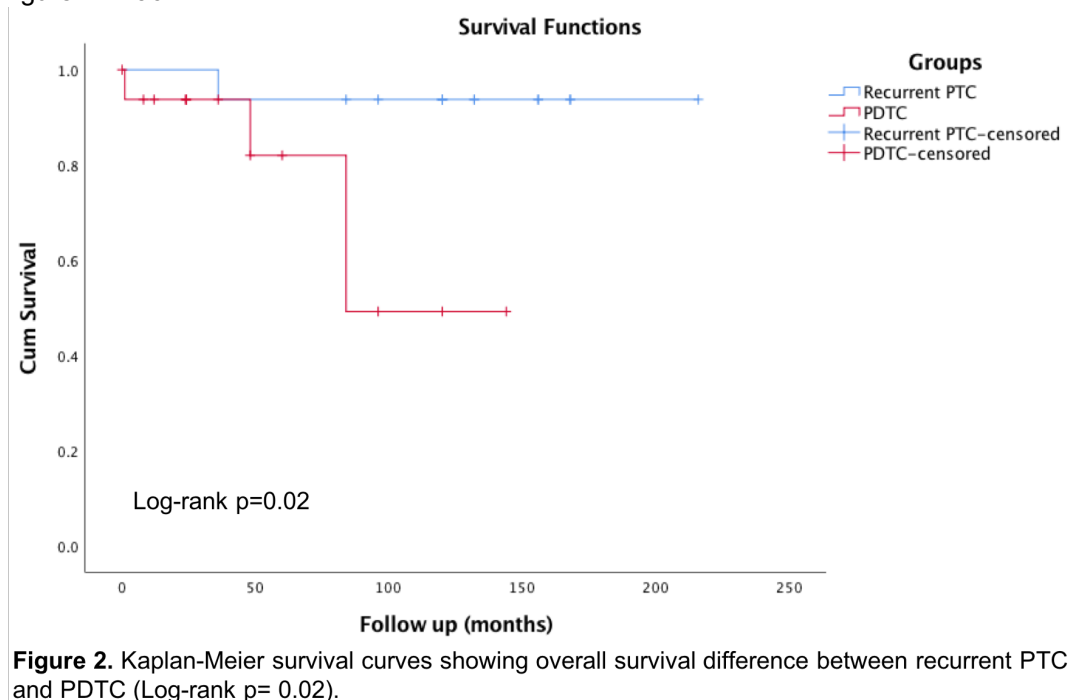


Figure 2. Kaplan-Meier survival curves showing overall survival difference between recurrent PTC and PDTC (Log-rank $p=0.02$).

Conclusions: The SLC5A5 and SLC5A8 5'-RRs hypomethylation correlate with the global hypomethylation status previously described in dedifferentiated thyroid tumors and precludes the use of demethylating agents in its treatment. Expression analysis is needed to explore if there is any relation between methylation status and mRNA levels of both genes in PDTC.

297 Utilization of ThyGenX/ThyraMIR Molecular Test on FNA of Indeterminate Thyroid Nodules- A Single Institution’s Experience

Zhengshan (Allen) Chen¹, Andrew Fong², Eugenia Hu³, Wafaa Elatre¹

¹LAC+USC Medical Center, Los Angeles, CA, ²University of Southern California, LAC+USC Medical Center, Los Angeles, ³University of Southern California, Keck School of Medicine of USC, Los Angeles, CA

Disclosures: Zhengshan (Allen) Chen: None; Andrew Fong: None; Eugenia Hu: None; Wafaa Elatre: None

Background: Thyroid nodules with fine-needle aspiration (FNA) showing atypia of undetermined significance (AUS) have a low risk of malignancy. Ancillary molecular testing has been recommended to further stratify risk of malignancy in those lesions. ThyGenX/ThyraMIR is a molecular test for oncogene mutations using next-generation sequencing (ThyGenX) that, when negative for the panel of BRAF, RET/PTC1, RET/PTC3, PAX8/PPAR, KRAS, HRAS, NRAS, and PIK3CA, is reflexed to a microRNA expression classifier (ThyraMIR). Here we report our experience using the ThyGenX/ThyraMIR molecular test on indeterminate thyroid nodules in the past 3 years.

Design: A retrospective study of 54 cases with indeterminate thyroid FNAs (45 with Bethesda category III, 8 with IV and 1 with V) was performed. One sample fixed with RNARetain or direct smear from each case was sent to Interpace for molecular testing. 11/54 cases had consequent thyroid resections. The molecular test results were correlated with the final histopathology.

Results: 34/54 (63%) cases had no mutations by ThyGenX. Among those 32 cases were negative, 1 was insufficient and 1 was positive by ThyraMIR. 15/54 (28%) cases had a RAS mutation by ThyGenX, 6 were negative and 9 were positive by ThyraMIR. 2/54 (4%) had a PARG-BMS1 fusion gene with 1 negative and 1 positive by ThyraMIR. 1/54 (2%) had a NCOA4-RET3 fusion gene. 1/54 (2%) had a BRAF V600E mutation. 1/54 (2%) had a BRAF K601E, and PTEN A126T mutation and was negative by ThyraMIR. In 11 cases with thyroidectomy, 6 were benign and 5 were malignant (Table 1). 3/6 benign cases were negative by both ThyGenX and ThyraMIR, 3 were positive for an NRAS mutation and positive by ThyraMIR. 1/5 malignant cases was negative by both ThyGenX and ThyraMIR, 4 were positive for a RAS mutation with 2 negative and 2 positive by ThyraMIR.

Table 1. Correlation between ThyGenX/ThyraMIR molecular test results and final resection diagnosis for indeterminate thyroid nodules

Case No.	TIRADS score	Cytology category	Interpace Diagnostics			Resection diagnosis
			ThyGenX	ThyraMIR	Interpretation	
Benign						
1	5	IV	No mutations	Neg	5% risk	Follicular hyperplasia
2	3	III	No mutations	Neg	5% risk	Follicular hyperplasia
3	3	III	No mutations	Neg	5% risk	Follicular hyperplasia
4	3	III	NRAS Q61K	Pos	45-60% risk	Adenomatoid nodule
5	2	III	NRAS Q61R	Pos	45-60% risk	Follicular adenoma
6	4	III	NRAS Q61R	Pos	45-60% risk	Follicular adenoma
Malignant						
7	5	III	No mutations	Neg	5% risk	FVPTC
8	4	III	NRAS Q61R	Neg	25-40% risk	PTC
9	5	III	NRAS Q61R	Neg	25-40% risk	PTC
10	3	III	NRAS Q61R	Pos	45-60% risk	PTC
11	3	III	HRAS Q61R	Pos	45-60% risk	FVPTC

FVPTC: follicular variant of papillary thyroid carcinoma; PTC: papillary thyroid carcinoma.

Conclusions: By using histological diagnosis as the gold standard in our study, the ThyGenX/ThyraMIR molecular test had a sensitivity of 80%, specificity of 50%, positive predictive value (PPV) of 57% and negative predictive value (NPV) of 75% for indeterminate thyroid nodules. Our results are consistent with published reports on ThyGenX/ThyraMIR. While this molecular test had a good NPV, PPV was suboptimal. Using this molecular test may help patients avoid unnecessary surgical procedures. However, the limitations of molecular testing have to be considered in managing indeterminate thyroid nodules.

298 Follicular Cells in Pituitary Neuroendocrine Tumors

Luvy Delfin Mendez¹, Ozgur Mete², Sylvia Asa¹

¹Case Western Reserve University/University Hospitals Cleveland Medical Center, Cleveland, OH, ²University Health Network, University of Toronto, Toronto, Canada

Disclosures: Luvy Delfin Mendez: None; Ozgur Mete: None; Sylvia Asa: *Advisory Board Member*, Leica Biosystems

Background: Follicular cells (FCs) are thought to be agranular, non-hormone producing stellate cells distributed throughout the adenohypophysis, occasionally arranged around colloid-filled follicles and thought to be more prominent in the vicinity of necrosis and apoptotic cells. A distinct but similar cell type, the folliculostellate cell (FSC), is a sustentacular cell that is negative for keratins and stains for S100, GFAP and SOX10. While several studies have examined FSCs in pituitary neuroendocrine tumors (PitNETs), the distribution and derivation of FCs in these lesions is unclear.

Design: The presence and distribution of FCs were studied in 100 PitNET cases obtained by trans-sphenoidal surgery, using immunohistochemistry for keratins as well as the full complement of immunohistochemical stains for tumor characterization.

Results: We examined 104 PitNETs including 9 somatotroph, 5 mammosomatotroph, 7 lactotroph, 7 poorly differentiated PIT1-lineage, 2 acidophil stem cell, 17 corticotroph, 53 gonadotroph, 2 null cell and 2 unusual plurihormonal tumors. CK-positive FCs were only identified in gonadotroph PitNETs and were found in 12 (23%) of those tumors; all other tumor types were negative for FCs. FCs express cytokeratins including CAM5.2, AE1/AE3 and CK19. FCs were identified scattered singly among hormone-producing endocrine cells, in small clusters of 3-5 cells and surrounding colloid-filled follicles, as well as linearly along blood vessels. Sequential stains showed that FCs also express nuclear SF1 and GATA3, transcription factors of gonadotrophs.

Conclusions: In our study series, FCs were exclusively found in gonadotroph PitNETs and occurred in 23% of those tumors. Co-expression of gonadotroph transcription factors in FCs supports the possible transformation of neoplastic hormone-producing cells to FCs. Further studies are required to determine if and why gonadotrophs alone undergo this transformation, the function of these cells and whether they have prognostic value.

299 Papillary Thyroid Microcarcinomas: Does Sub-Typing Predict Aggressive Clinical Behavior?

Maria Gubbiotti¹, Virginia LiVolsi², Zubair Baloch¹

¹Hospital of the University of Pennsylvania, Philadelphia, PA, ²University of Pennsylvania, Philadelphia, PA

Disclosures: Maria Gubbiotti: None; Virginia LiVolsi: None; Zubair Baloch: None

Background: Papillary thyroid microcarcinomas (PTCMCs) comprise a set of indolent tumors measuring ≤ 1.0 cm. This study examines whether the morphologic sub-type of PTCMCa correlates with clinical behavior.

Design: The pathology database at our institution was searched between the years of 2009-2020 for cases of PTCMCa. Information extracted from the reports included patient demographics, number of foci, presence or absence of capsular or lymphovascular invasion, extrathyroidal extension, and lymph node metastases. Chi-square tests were utilized to evaluate statistical significance.

Results: The case cohort included 300 cases of classic variant (PTCMCa-CV), 758 of follicular variant (PTCMCa-FV), 217 of tall cell variant (PTCMCa-TCV), and 5 of Warthin-like variant (PTCMCa-WV). All tumors ranged in size from 0.1-1.0 cm and all had female predominance (PTCMCa-CV M:F = 70:181, PTCMCa-FV M:F = 149:473, PTCMCa-TCV M:F = 57:156, PTCMCa-WV M:F = 1:4). A statistically significant age difference at first presentation was noted between PTCMCa-TCV and PTCMCa-CV (52.0 vs. 48.4 years), however, none was noted between PTCMCa-TCV and PTCMCa-FV. PTCMCa-TCV was associated with significantly greater rates of extrathyroidal extension (ETE) and lymph node metastases than either PTCMCa-CV or PTCMCa-FV and significantly greater rates of lymphovascular invasion (LVI) than PTCMCa-FV. Of the 5 PTCMCa-WV, none showed ETE, LVI, or lymph node metastases. (see Table 1).

	<i>PTCMCa-CV</i>	<i>PTCMCa-FV</i>	<i>PTCMCa-TCV</i>	<i>PTCMCa-WV</i>	<i>p value*</i>
Age (years)	<45: 114	<45: 227	<45: 70	<45: 1	CV vs. TCV: 0.03
	>45: 159	>45: 446	>45: 148	>45: 4	FV vs. TCV: 0.66
	Mean: 48.4	Mean: 52.0	Mean: 52.0	Mean: 47.4	
Sex	M: 70 F: 181	M: 149 F: 473	M: 57 F: 156	M: 1 F: 4	CV vs. TCV: 0.79
					FV vs. TCV: 0.41
Tumor capsule invasion	Yes: 46 (70.8%)	Yes: 58 (50%)	Yes: 12 (20.3%)	Yes: 1 (25%)	CV vs. TCV: <0.0001
	No: 19 (29.2%)	No: 58 (50%)	No: 47 (79.8%)	No: 3 (75%)	FV vs. TCV: 0.00015
Extrathyroidal extension	Yes: 33 (11.2%)	Yes: 28 (4.8%)	Yes: 79 (39.3%)	Yes: 0 (0%)	CV vs. TCV: <0.0001
	No: 261 (88.8%)	No: 551 (95.2%)	No: 122 (60.7%)	No: 3 (100%)	FV vs. TCV: <0.0001
Foci	Multiple: 184	Multiple: 416	Multiple: 132	Multiple: 4	CV vs. TCV: 0.91
	Single: 116	Single: 342	Single: 85	Single: 1	FV vs. TCV: 0.12
Lymphovascular invasion	Yes: 98 (32.7%)	Yes: 75 (15.3%)	Yes: 22 (42.3%)	Yes: 0 (0%)	CV vs. TCV: 0.18
	No: 202 (67.3%)	No: 414 (84.7%)	No: 30 (57.7%)	No: 5 (100%)	FV vs. TCV: <0.00001
Lymph node metastasis	Yes: 107 (36.0%)	Yes: 109 (16.9%)	Yes: 80 (48.1%)	Yes: 0 (0%)	CV vs. TCV: 0.01
	No: 190 (63.9%)	No: 537 (83.1%)	No: 86 (51.8%)	No: 4 (100%)	FV vs. TCV: <0.00001

Key:

PTCMCa-CV: Papillary thyroid carcinoma-classic variant

PTCMCa-FV: Papillary thyroid carcinoma-follicular variant

PTCMCa-TCV: Papillary thyroid carcinoma-tall cell variant

PTCMCa-WV: Papillary thyroid carcinoma-Warthin variant

*Due to the small sample size, PTCMCa-WV was not included in the statistical analysis.

Conclusions: Our data support PTCMCa-TCV as a more aggressive variant of PTCMCa when compared with PTCMCa-CV and PTCMCa-FV. Even though our sample size for PTCMCa-WV is small, these PTCMCas appear to follow a less aggressive path. Therefore, we recommend histologic subtyping of PTCMCa as there is a difference in clinical behavior among the different groups.

300 Thyroid Nodules with Copy Number Alterations: A Genotypic-Phenotypic Correlation

Amin Heidarian¹, Bruce Wenig¹, Juan Hernandez-Prera¹
¹H. Lee Moffitt Cancer Center & Research Institute, Tampa, FL

Disclosures: Amin Heidarian: None; Bruce Wenig: None; Juan Hernandez-Prera: None

Background: ThyroSeq v3 genomic classifier introduced the detection of DNA copy number alterations (CNA), which have been associated with Hürthle cell phenotype. Herein, we present a study focusing on the clinicopathologic features of thyroid nodules with CNA.

Design: Institutional records were searched for cases of thyroid nodules subjected to ThyroSeq V3 analysis that reported CNA. The cytology and molecular results were correlated with their corresponding surgical resections when available.

Results: Twenty-eight nodules with CNA were identified and 7 of them had additional mutations (1 *TP53*, 1 both *TP53* and *RAS*, 4 *RAS*, and 1 *PTEN*). Cases included 19 women and 9 men, with a median age of 60 years (range 31-82). The Bethesda (B) category distribution was 10 follicular lesions of undetermined significance (FLUS) (B III), 16 follicular neoplasms (B IV) [including 10 oncocyctic and 6 non-oncocyctic], 1 suspicious for malignancy (B V), and 1 malignant (B VI) [anaplastic thyroid carcinoma (ATC)]. Fourteen nodules underwent surgery with a mean tumor size of 2.76 cm (range 1.7-7 cm). Nine were benign [4 hyperplastic nodules (HN), 5 follicular adenomas (FA)], 2 were noninvasive follicular thyroid neoplasms with papillary-like nuclear features (NIFTP), and 3 were malignant [2 follicular thyroid carcinomas (FTC) and 1 poorly-differentiated thyroid carcinoma (PDTC)]. One FTC showed high-grade features characterized by 7 mitoses per 10 high-power field (HPF) but no necrosis or solid growth pattern; the PDTC was encapsulated and non-invasive. Nodules composed of ≥ 75% of oncocyctic cells were classified as Hürthle cell lesions (1 HN, 3 FA, 2 FTC, and 1 PDTC), however, the remainder of nodules showed cytoplasmic changes with eosinophilia but did not show the brightly eosinophilic and granular cytoplasm defining true oncocyctic cells. The PDTC and ATC had co-existing *TP53* mutations and 1 NIFTP had a *RAS* mutation.

Conclusions: Thyroid nodules with CNA appear to occur in older patients with the majority exhibiting follicular architecture and frequent oncocyctic morphology on cytology and in surgical specimens. However, their designation as a Hürthle cell lesion should be established only after examination of the surgical specimen and the diagnosis of malignancy is (mostly) predicated on the presence of invasion. The co-existence of *TP53* mutation was associated with high risk of cancer. Nodules that did not meet the 75% of oncocyctic cells still showed cytoplasmic changes challenging the validity of this arbitrary diagnostic cut-off.

301 Moleculars Alterations in Radioiodine Therapy Resistant Thyroid Carcinomas

Myriam Kossai¹, Camille Darcha¹, Marie-Celeste Ferreira¹, Anne Cayre¹, Lucie Tixier¹, Beryl Bayol¹, Genevieve Fouilhoux², Florence Mishellany¹, Antony Kelly¹, Frederique Penault-Llorca¹
¹Centre Jean Perrin, Clermont Ferrand, France, ²CRLCC Jean Perrin, Clermont-Ferrand, France

Disclosures: Myriam Kossai: None; Camille Darcha: None; Marie-Celeste Ferreira: None; Anne Cayre: None; Lucie Tixier: None; Antony Kelly: None; Frederique Penault-Llorca: *Consultant*, Lilly; *Consultant*, Bayer; *Grant or Research Support*, Bayer; *Grant or Research Support*, Roche; *Consultant*, Roche

Background: Differentiated thyroid cancers (DTC) represent the vast majority of thyroid cancers (TC), they are sensitive to radioactive iodine therapy and associated with a good prognosis. However, a small proportion of cases with a locally advanced disease or distant metastases will become radioactive iodine (RAI) refractory with a pejorative prognosis as well as some histologic subtypes of TC such as anaplastic (ATC) and medullary (MTC) tumors. The recent understanding of the molecular alterations and mechanisms in tumors is essential in order to provide potential targeted therapy to the patients. The aim of this study is to identify molecular alterations in a large cohort of thyroid carcinoma especially in RAI-refractory thyroid cancers and aggressive histological and clinical subtypes.

Design: This unicentric and retrospective study included 152 patients treated for thyroid cancer between 1995 and 2019. Using tumor samples of the entire cohort, tissue microarrays were built. Immunohistochemical analysis was

performed using TRK A/B/C (EPR17341), ALK (5A4) and PD-L1 (SP263) antibodies. RNA based analysis using a targeted panel of mutations and rearrangements (FusionPlex Comprehensive Thyroid and Lung kit, Archer DX) was also conducted.

Results: Heifty-six cases were sequenced. Fifty-two point mutations (60.5%) notably in BRAF, RET, RAS genes were identified as well as 2 gene fusions involving NTRK and ALK genes. There was a poor correlation between NTRK protein expression and NRTK alterations found by RNA sequencing data. The ALK fusion case shown ALK protein expression. Regarding the number of genomic alterations between RAI-refractory and RAI-non refractory TC, there was no significant difference ($p=0.5$). PD-L1 expression was highly expressed in tumor cells in aggressive type of thyroid cancers, in 58.3% of ATC and 62.5% of poorly differentiated carcinomas (PDTC).

Conclusions: Molecular alterations can be effectively identified routinely in formalin-fixed paraffin-embedded (FFPE) tissue samples. Patients presenting thyroid tumors with targetable alterations could be eligible for specific therapy such as larotrectinib or entrectinib targeting *NTRK* fusion or selpercatinib and pralsetinib targeting *RET* fusion. Immunotherapy alone or in combination with other drugs may be a promising treatment for aggressive types of thyroid cancers.

302 lncRNA Expression and SDHB Mutation in Pheochromocytomas and Paragangliomas (PPGLs)

Hui-Hua Li¹, Heather Hardin², Misbah Zaeem², Wei Huang², Rong Hu¹, Ricardo Lloyd²

¹University of Wisconsin School of Medicine and Public Health, Madison, WI, ²University of Wisconsin, Madison, WI

Disclosures: Hui-Hua Li: None; Heather Hardin: None; Misbah Zaeem: None; Wei Huang: None; Rong Hu: None; Ricardo Lloyd: None

Background: Although most pheochromocytomas and paragangliomas (PPGLs) are often low grade neoplasms, the metastatic forms of these lesions are associated with high morbidity and mortality. Recent studies have discovered multiple aberrantly expressed long non-coding RNAs (lncRNAs) in cancers that may have regulatory roles in tumor pathogenesis and metastasis; however, the roles of some lncRNAs in PPGLs are still unknown. Immunohistochemistry with an anti-SDHB antibody can be used to detect mutations with loss of expression of SDHx in PPGLs and in the PPGL syndrome.

Design: The expression levels of lncRNAs including metastasis-associated lung adenocarcinoma transcript (*MALAT1*), prostate cancer antigen 3 (*PCA3*), and HOX transcript antisense intergenic RNA (*HOTAIR*) in PPGLs were analyzed by in situ hybridization, using two tissue microarrays (TMAs). The pheochromocytoma (P) TMA consisted of normal adrenal medulla (N=25), non-metastatic Ps (N=76) and metastatic Ps (N=5) while the paraganglioma (PGL) TMA had 73 non-metastatic PGLs and 5 metastatic PGLs. Immunohistochemical staining was performed in all samples with an anti-SDHB antibody. The correlations among lncRNA expression, loss of SDHB expression and clinical characteristics including tumor progression and disease prognosis were investigated.

Results: The expression levels of *MALAT1* and *PCA3* were significantly elevated (2.5-3.9 folds) in both non-metastatic and metastatic Ps compared to normal adrenal medulla, although there were no significant differences between the non-metastatic and metastatic groups. However, in contrast to non-metastatic PGLs, metastatic PGLs had significantly upregulated expression of *MALAT1*, *PCA3*, and *HOTAIR*. SDHB loss was more frequently observed in PGLs (25 of 78) and especially in metastatic PGLs (5 out of 5), compared to Ps (2 of 81) and in 0 of 5 metastatic Ps. Patients with SDHB loss, in contrast to SDHB retained were younger at diagnosis (39 vs. 51 years of age), also had higher rates of tumor recurrence (32% vs. 6%), metastatic disease (20% vs. 0%), and mortality (16% vs. 0%). In addition, the group with SDHB loss also had significantly increased expression level of *PCA3* (as well as a trend towards increased *MALAT1* and *HOTAIR*) compared to the group with intact SDHB expression.

Conclusions: The lncRNAs *MALAT1*, *PCA3*, and *HOTAIR* are upregulated in metastatic PPGLs. SDHB loss in PGLs is associated with increased expression of *PCA3*. In addition, SDHB loss is a useful marker to predict poor prognosis in PGLs.

303 Severe Obesity is Associated with Pituitary Corticotroph Hyperplasia. Cause or Consequence?

Riley Lochner¹, Luvy Delfin Mendez², Behtash Nezami³, Sylvia Asa², Mark Cohen⁴, Bartolome Burguera⁵, Marta Couce⁶

¹University Hospitals of Cleveland, Case Western Reserve University, Cleveland, OH, ²Case Western Reserve University/University Hospitals Cleveland Medical Center, Cleveland, OH, ³The University of Texas MD Anderson Cancer Center, Houston, TX, ⁴University Hospitals of Cleveland, National Prion Disease Pathology Surveillance Center, ⁵Cleveland Clinic, Cleveland, OH, ⁶University Hospitals Cleveland Medical Center, Cleveland, OH

Disclosures: Riley Lochner: None; Luvy Delfin Mendez: None; Behtash Nezami: None; Sylvia Asa: Advisory Board Member, Leica Biosystems; Mark Cohen: None; Bartolome Burguera: None; Marta Couce: None

Background: The link between obesity and chronic systemic inflammation with hyperactivation of the hypothalamic-pituitary axis by pro-inflammatory cytokines is well established. Elevated serum ACTH has been correlated with excess body weight, especially in relation to Cushing disease. Yet, little is known about the incidence of hypophysitis in the general population or its prevalence in obesity. Similarly, the incidence of corticotroph hyperplasia in obesity has never been systematically studied. Thus, we examined the prevalence of hypophysitis and corticotroph hyperplasia in our autopsy population.

Design: We retrospectively reviewed the histopathology of one hundred sixty-one pituitaries removed from adult subjects at the time of autopsy between 2010 and 2018 at UH Cleveland Medical Center. The clinical history, body mass index (BMI), and cause of death were recorded. H&E, reticulin, and immunohistochemical stains for ACTH, CD3, and CD20 were reviewed by two pathologists. The data were analyzed using Fisher and Chi-square statistics.

Results: Decedents were separated into 4 groups based on BMI (kg/m²): Lean (BMI <25.0), overweight (BMI of 25.0 to 29.9), obesity class I (BMI of 30.0 to 34.9), and (severe) obesity class II (BMI >34.9). Microscopic foci of T lymphocytes and B lymphocytes were identified in each weight category, as well as corticotrophin hyperplasia (identified in 44 of 161 pituitary glands, Table 1). Pituitaries with corticotrophin hyperplasia were then reexamined for T cell and B cell inflammation. Of the 44 cases of hyperplasia, 40 (90.9%) had microscopic foci of T cell inflammation and 12 (27.2%) had microscopic foci of B cell inflammation, compared with 54 (46.2%) (p<0.0001) and 10 (8.5%) (p=0.0021) pituitaries without corticotroph hyperplasia, respectively.

		Overall	Weight Category			
			Lean	Overweight	Obesity I	Obesity II
T-cell Inflammation	No	67	32.9%(53)	21.7%(35)	17.4%(28)	28%(45)
	Yes	94	40.3%(27)	13.4%(9)	16.4%(11)	29.9%(20)
	p-value	0.1244	27.7%(26)	27.7%(26)	18.1%(17)	26.6%(25)
B-cell Inflammation	No		33.8%(47)	20.9%(29)	16.5%(23)	28.8%(40)
	Yes		27.3%(6)	27.3%(6)	22.7%(5)	22.7%(5)
	p-value	0.7359				
Corticotroph Hyperplasia	No	117	41.9%(49)	19.7%(23)	15.4%(18)	23.1%(27)
	Yes	44	9.1%(4)	27.3%(12)	22.7%(10)	40.9%(18)
	p-value	<0.0001				

Table 1. Prevalence of T-cell and B-cell inflammation and corticotroph hyperplasia by weight category

Conclusions: We found a significant association between severe obesity and corticotroph hyperplasia as well as between corticotroph hyperplasia and adenohypophysitis. We found no independent association between BMI and hypophysitis. These findings support the possibility that corticotroph hyperplasia could induce a sub-clinical Cushing-like syndrome that contributes to increased appetite, metabolic abnormalities, and obesity. It is unknown if corticotroph hyperplasia is a response to adenohypophysitis. The clinical significance of these findings is uncertain. Additional investigations will be necessary to discern whether corticotrophin hyperplasia plays a causal role in the development of obesity.

304 Evaluation of Grade in a Genotyped Sporadic Medullary Thyroid Carcinoma Cohort

Fedaa Najdawi¹, Justine Barletta¹

¹Brigham and Women's Hospital, Harvard Medical School, Boston, MA

Disclosures: Fedaa Najdawi: None; Justine Barletta: None

Background: Tumor grade and genotype have been reported to be prognostic in sporadic medullary thyroid carcinoma (MTC); however, the association between grade and genotype has not been evaluated. The aim of this project was to evaluate grade in a genotyped sporadic MTC cohort.

Design: We identified 25 sporadic MTC with molecular analysis previously performed (cohort will be expanded by the time of presentation). For each case, we evaluated all tumor slides available and recorded mitotic count per 10 high power fields (HPF) and the presence of tumor necrosis. Ki-67 was performed, and the Ki-67 proliferative index (PI) was determined in the area of highest proliferative activity (500-2000 cells counted). The grade was assigned according to two recently published studies, which we termed grading scheme (GS)1 and GS2, see Tables 1 and 2. Tumor genotype was risk stratified as follows: tumors with RET mutations in exons 15 and 16 (which includes the RET Met918Thr mutation) were designated high risk, and tumors with other RET mutations, RAS mutations, or a wild-type RET/RAS status were designated low to intermediate risk.

Table (1) Grading Scheme (GS)1

Grade	Mitotic Count per 10 HPF	Coagulative Necrosis
Low	<5	Absent
High	<5	Present
High	≥5	Present or absent

Table (2) Grading Scheme (GS)2

Grade	Mitotic Count per 10 HPF	Ki-67 Proliferative Index (%)	Coagulative Necrosis
Low	<3	<3	Absent
Intermediate	<3	<3	Present
Intermediate	3-20	3-20	Absent
High	3-20	3-20	Present
High	>20	>20	Present or absent

Results: Using GS1, 19 tumors were low grade and 6 tumors were high grade. GS2 classified 18 tumors as low grade, 3 as intermediate grade, and 4 as high grade. Of the 7 tumors that had a high-risk genotype (including 6 with the RET Met918Thr mutation), all were GS1 low grade. Utilizing GS2, 6 were low grade and 1 was intermediate grade. The 18 tumors with a low to intermediate risk genotype included 3 with low-risk RET mutations, 4 with an HRAS mutation, 3 with a KRAS mutation, 1 with both HRAS and KRAS mutations, and 7 tumors that were wild-type for RET and RAS. For the low to intermediate-risk genotype group, 12 were GS1 low grade and 6 were GS1 high grade. Utilizing GS2, 12 were low grade, 2 were intermediate grade, and 4 were high grade. Of the high-grade tumors using either grading system, none had a high-risk RET mutation, 2 had low-risk RET mutations, 1 had an HRAS mutation, and 3 were wild-type for RET and RAS.

Conclusions: In our cohort, high-grade tumors lacked high-risk RET mutations, suggesting that grade and genotype may give independent prognostic information.

305 NRAS Q61R Immunohistochemical Staining (IHC) in Thyroid Pathology: Sensitivity, Specificity and Utility

Maëlle Saliba¹, Nora Katabi¹, Snjezana Dogan¹, Ronald Ghossein¹, Bin Xu¹

¹Memorial Sloan Kettering Cancer Center, New York, NY

Disclosures: Maëlle Saliba: None; Nora Katabi: None; Snjezana Dogan: None; Ronald Ghossein: None; Bin Xu: None

Background: The diagnosis and subtyping of thyroid neoplasms relies on the demonstration of histologic parameters that can be focal and prone to subjective interpretation. We aimed to study the utility of NRAS Q61R IHC in the diagnosis of thyroid lesions and determine its specificity and sensitivity as a surrogate marker for underlying RAS mutation.

Design: NRAS Q61R IHC was performed on 282 nodules from 256 patients. RAS mutation status was collected from patients' chart when available. Sensitivity and specificity of NRAS Q61R IHC for detecting a RAS Q61R mutation was calculated. IHC-positive cases were reviewed by three pathologists to determine the diagnostic utility of NRAS Q61R IHC.

Results: The rates of positive NRAS Q61R IHC per diagnostic category are listed in table 1. In total, 84 lesions (29.8%) received molecular testing assessing RAS driver mutations. NRAS Q61R antibody cross-reactivity resulted in a detection of NRAS Q61R, KRAS Q61R and HRAS Q61R proteins. RAS Q61R mutations were identified in 38.1% of tested cases (20 cases showing mutated NRAS Q61R, 8 showing mutated HRAS Q61R and 4 showing mutated KRAS Q61R). The sensitivity and specificity of NRAS Q61R IHC in detecting RAS Q61R mutation was 90.6% and 92.3%, respectively. Three of four false positive lesions showed oncocytic changes. When positive, the NRAS Q61R stain was determined to be helpful in the pathologic diagnosis of thyroid lesions in 86.4% of cases, alternatively aiding in highlighting infiltrative (n=11) or well-circumscribed (n=31) tumor borders, identifying satellite nodules as capsular invasion (n=21), confirming vascular invasion (n=1), determining multifocality (n=3), demarcating the entirety of the lesion for accurate size assessment (n=2) and confirming the thyroid origin of a metastasis (n=1).

Table 1- Rates of positive NRAS Q61R IHC per diagnostic category

Diagnosis	Number of positive cases/Number of all cases tested (%)
Non-neoplastic	2/11 (18.2%)
Nodular hyperplasia	2/10 (20.0%)
Thyroid remnant	0/1 (0%)
Benign	2/9 (22.2%)
Follicular adenoma	1/5 (20.0%)
Hurthle cell adenoma	1/3 (33.3%)
Hyalinizing trabecular tumor	0/1 (0%)
Noninvasive follicular thyroid neoplasm with papillary-like nuclear features	28/67 (41.8%)
Malignant	50/195 (25.6%)
Primary	47/183 (25.7%)
Anaplastic carcinoma	2/6 (33.3%)
Poorly differentiated carcinoma	4/16 (25.0%)
Papillary carcinoma	40/148 (27.0%)
Follicular variant	37/79 (46.8%)
Infiltrative	11/22 (50.0%)
Encapsulated	26/57 (45.6%)
Classic	2/60 (3.3%)
Tall cell variant	0/4 (0%)
Solid variant	1/5 (20.0%)
Follicular carcinoma	1/7 (14.3%)
Hurthle cell carcinoma	0/6 (0%)
Metastasis	3/12 (25.0%)
Anaplastic carcinoma	0/4 (0%)
Poorly differentiated carcinoma	3/6 (50.0%)
Hurthle cell carcinoma	0/1 (0%)
Papillary carcinoma	0/1 (0%)

Conclusions: The NRAS Q61R IHC is a highly sensitive and specific marker for the detection of the RAS Q61R mutations in thyroid pathology. When evaluated in adjunction with histologic features, NRAS Q61R immunoreactivity can be a helpful ancillary tool for achieving the correct diagnosis and classification of thyroid nodules.

306 Clinicopathologic and Prognostic Features of Follicular-Cell Derived Pediatric Thyroid Carcinomas: A Study of 182 Cases from a Single Institution

Maelle Saliba¹, Bayan Alzumaili², Nora Katabi¹, Snjezana Dogan¹, Bin Xu¹, Ronald Ghossein¹
¹Memorial Sloan Kettering Cancer Center, New York, NY, ²Mount Sinai Health System, New York, NY

Disclosures: Maelle Saliba: None; Bayan Alzumaili: None; Nora Katabi: None; Snjezana Dogan: None; Bin Xu: None; Ronald Ghossein: None

Background: Thyroid malignancies are rare in pediatric patients and are mainly approached based on data extrapolated from adults. We report the clinicopathologic and prognostic features of pediatric follicular cell-derived thyroid carcinomas (TC) followed at a single referral center.

Design: We retrospectively reviewed 182 pediatric TCs (patient age ≤21 years) diagnosed from 1988 to 2018. The volume of lymph node (LN) disease at primary resection was considered as high if the largest positive LN measured ≥ 1 cm and/or 5 or more LNs were positive. Poorly differentiated TCs (PDTC) were defined using our institutional criteria and considered as high-risk histology along with diffuse sclerosing variant (DSV) papillary thyroid carcinomas (PTC). Disease, locoregional recurrence and distant metastasis free survival (DFS, LRFS and DMFS) were analyzed for all TCs using univariate log rank test and multivariate Cox proportional hazards model.

Results: Clinicopathologic characteristics are summarized in table 1. LN involvement at presentation was significantly associated with male sex, no or partial tumor encapsulation, and lymphovascular invasion (LVI) by Pearson's chi-square test (p<0.05). Of 13 patients with distant disease, 9 (69%) initially presented with metastases. Both DSV and PDTC significantly correlated with a larger primary (p<0.05). In addition, DSV also correlated with positive margins and high-volume nodal disease at presentation (p<0.05). DSV, but not tall cell PTC, significantly predicted worse DFS and LRFS, whereas PDTC significantly imparted worse DMFS (p<0.05). By univariate analysis, large tumor size, lack of complete encapsulation, LVI, positive surgical margin and positive LN at presentation were all significant predictors of worse DFS (p<0.05). In addition, male sex was a significant predictor of DMFS (p<0.05). By multivariate analysis, PDTC and tumor size independently predicted DFS while PTDC was the only independent factor for DMFS. 5-year and 10-year DFS was 90% and 84% respectively. Only one patient with PDTC died of disease.

Table 1. Patients' clinicopathologic characteristics

Characteristic	n=182	% of total
Median age at diagnosis, years (range)	16.8 (2.7-21.8)	
Median follow-up, years (range)	6.3 (0-29.6)	
Gender (n=182)		
Female	144	79.1
Male	38	20.9
Tumor size, cm (n=182)		
<4	144	79.1
≥4 cm	38	20.9
Encapsulation (n=182)		
Partial/none	141	77.5
Complete	41	22.5
Capsular invasion* (n=41)		
None	19	46.3
Focal	17	41.5
Extensive	5	12.2
Lymphovascular invasion (n=182)		
None	104	57.1
Focal	35	19.2

Extensive	43	23.6
Gross extrathyroidal extension (n=182)		
Absent	171	95.0
Present	9	5.0
Surgical margins (n=182)		
Negative	142	79.8
Positive	36	20.2
Histology (n=182)		
Follicular carcinoma	4	2.2
Hurthle cell carcinoma	1	0.5
Papillary thyroid carcinoma		
Follicular variant		
Infiltrative	2	1.1
Encapsulated	9	4.9
Classic type	86	47.3
Cribiform morular variant	1	0.5
Tall-cell variant	31	17.0
Solid variant	2	1.1
Diffuse sclerosing variant	19	10.4
Poorly differentiated carcinoma	27	14.8
Lymph node status at presentation (n=182)		
N0	69	37.9
N1	113	62.1
Stage at presentation (n=180)		
T1	171	95.0
T2	9	5.0

* For completely encapsulated tumors

Conclusions: While pediatrics TCs have a good prognosis overall, large unencapsulated tumors, male sex, and PDTC are associated with a protracted course of disease. DSV, but not tall cell PTC, constituted an aggressive variant of PTC. Accurate recognition of DSV and PDTC are important for risk stratification in the pediatric patient population.

307 Characterizing Pathologic Response Following Neoadjuvant Targeted Therapy in BRAFV600E Mutated Anaplastic Thyroid Carcinoma

Linton Sellen¹, Yelda Jozaghi¹, Diana Bell¹, Maria Cabanillas¹, Ramona Dadu¹, Mark Zafereo¹, Michelle Williams¹

¹The University of Texas MD Anderson Cancer Center, Houston, TX

Disclosures: Linton Sellen: None; Yelda Jozaghi: None; Diana Bell: None; Maria Cabanillas: None; Ramona Dadu: None; Mark Zafereo: Grant or Research Support, Merck, Eli Lilly; Advisory Board Member, Eli Lilly; Michelle Williams: None

Background: Anaplastic thyroid carcinoma (ATC) is a deadly disease often arising as dedifferentiation from BRAFV600E mutated papillary thyroid carcinoma (PTC). Recent FDA approval for combined BRAF and MEK inhibitor therapy in ATC patients has resulted in meaningful surgical resection following marked tumor reduction in previously borderline/non-resectable patients. When feasible, surgical resection appears to impact survival. The histologic changes associated with targeted therapy has not been characterized nor detailed in association with degree of response. Our goal is to pathologically characterize the tumor, stromal and immune response post neoadjuvant therapy in the thyroid specimens.

Design: Surgical specimens were histologically reviewed from 19 patients with BRAFV600E mutated ATC who received targeted BRAF/ MEK inhibitor therapy with (15) or without immunotherapy (4) from 2017-2020. Pathologic features of the thyroid post neoadjuvant therapy were characterized for extent of residual ATC and coexisting PTC, type of stromal changes (hyalinized versus proliferative immature fibrosis), necrosis, and degree of background inflammatory components by H & E slide review. Associations between pathologic features and extent of response, complete (CR) versus partial response (PR) in the thyroid, were evaluated.

Results: Residual ATC was present in 6 (32%) thyroids all with concomitant PTC, 12 (63%) with only PTC remaining and 1 showed no residual ATC or PTC. Marked mixed stromal changes (hyaline and immature fibrosis) were present. Prominent necrosis with macrophage response was present in 5 (26%) (Figure 1) and hemosiderian in 15 (79%). Tumor infiltrating lymphocytes (TILs) and/or mixed stromal inflammation was variably present in 17 (89%) (Figure 2). Grouping the histologic findings into 3 phenotypes noted ATC PR was more commonly associated with higher inflammation (TILs) and/or necrosis and ATC CR in thyroids with lower inflammation (Table).

Histopathologic findings in neoadjuvant treated BRAFV600E ATC surgical thyroid specimens and response

	19 total	Findings	Response				Stromal changes		Inflammation	
			# ATC CR	# ATC PR	% viable tumor	# PTC	Hyaline	Immature	Necrosis/ macrophages	TILs/ stromal inflammation
I	5 (26%)	Tumor necrosis; macrophage response	3	2	<5%, 70%	5	+	++	High	Mod-High
II	5 (26%)	Inflammatory Higher Cellularity	1	4	<15%	5	++	++	Rare	High
III	9 (47%)	Repair/ Resolving	9	0	n/a	8	++	+	No	Low

ATC=Anaplastic thyroid carcinoma; CR=Complete Response, PR=Partial Response; PTC=Papillary thyroid carcinoma; TILs=tumor infiltrating lymphocytes.

Figure 1 - 307

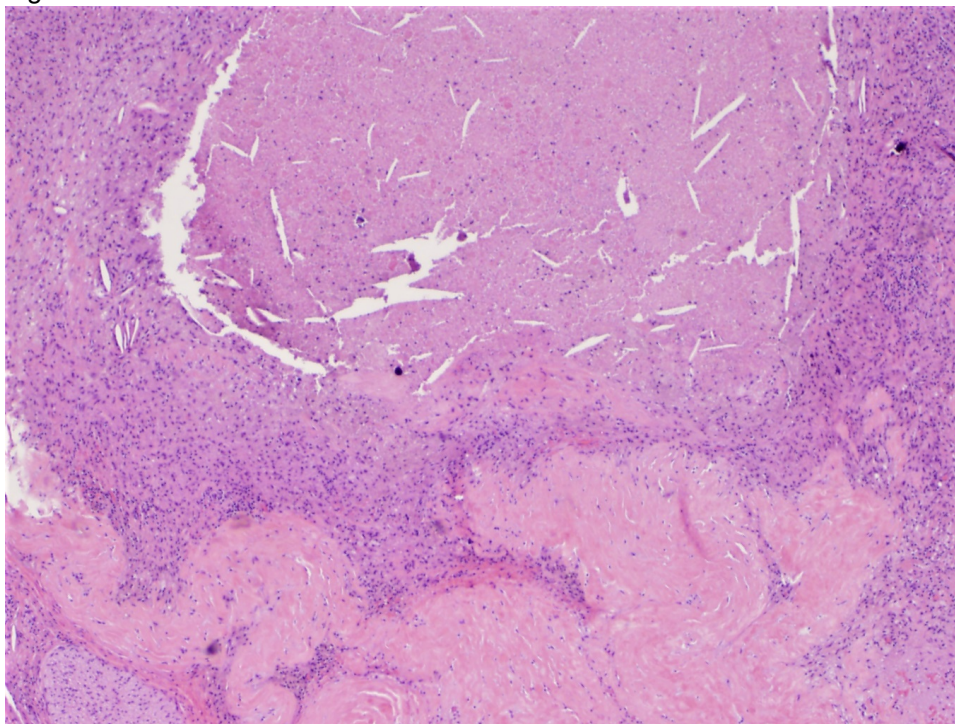
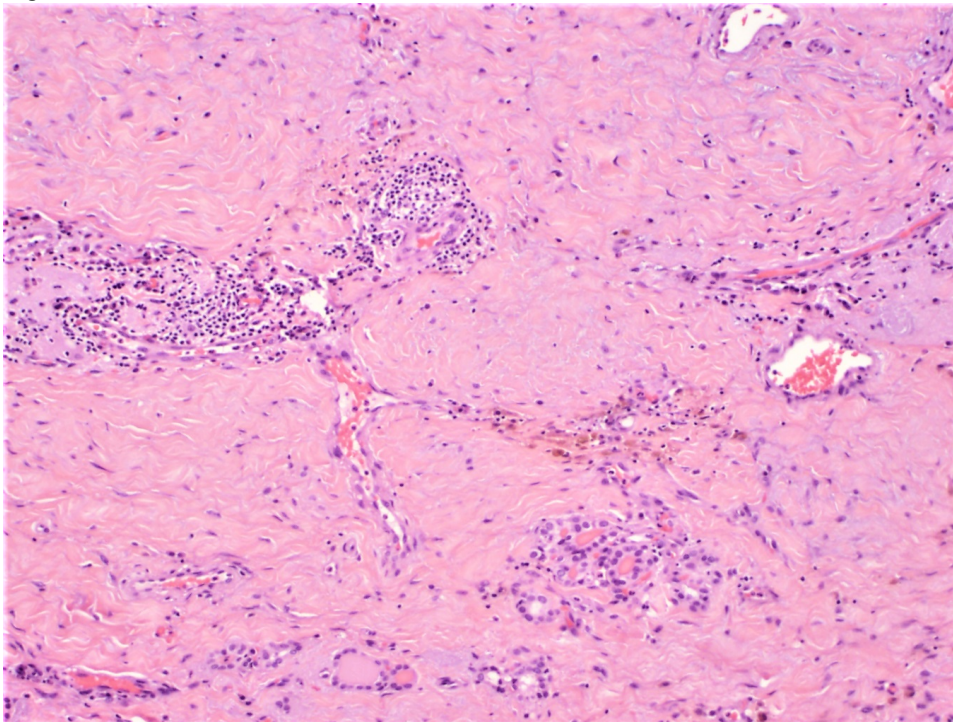


Figure 2 - 307



Conclusions: Dramatic resolution of ATC following neoadjuvant targeted therapy resulted in thyroid tumor bed stromal fibrosis and variable degree of inflammation/TILs. Lower cellularity was associated with complete ATC response in the thyroid. However, residual PTC was nearly universal following neoadjuvant therapy. Further correlations with duration of therapy and coexisting mutations is warranted.

308 Leaving No Carcinoma Behind! (If Possible)

Orhan Semerci¹, Hasan Gucer¹

¹Recep Tayyip Erdoğan University School of Medicine, Rize, Turkey

Disclosures: Orhan Semerci: None; Hasan Gucer: None

Background: Thyroid carcinoma incidence has been increasing over the decades and it is expected to increase more thanks to our ability to detect even smaller microcarcinomas. Although papillary microcarcinomas (PMCs) are considered mostly as 'innocent' because of their occult clinical course, they can recur, metastasize and they may cause morbidity and even mortality in some cases. Our aim was to investigate the presence and frequency of microcarcinomas we left behind in gross thyroidectomy materials despite our extremely careful macroscopic evaluation.

Design: Cases were included in the study if they displayed 1) a preoperative diagnosis of multinodular goiter 2) had a 'benign' fine needle aspiration pathology report prior to surgery 3) had no detectable intra-parenchymal primary carcinoma after microscopic evaluation of routine first sampling (at least one representative section from every one of the individual nodules and from any abnormality seen grossly). A total of seventy-two total thyroidectomy cases fulfilling the above criteria were randomly selected and included in the study in a prospective manner starting from the year 2014 to 2019. We then sampled the all remaining material (second sampling, whole gland) and reviewed corresponding histology slides, and finalized sign-outs. We also compared the relationship between clinicopathological features of cases with and without detected carcinomas after sampling the entire gland.

Results: We identified 1038 papillary thyroid carcinomas (%48.7) and 594 incidental papillary microcarcinomas (%27.8) (Figure 1) and 2 incidental medullary microcarcinomas (%0.001) out of 2130 total thyroidectomy cases in our institute during the 2014-2019 period upon research from the electronic health records system. Our first routine

grossing resulted in sampling 1 block per 3.80 gr of thyroid tissue and second grossing resulted in sampling 1 block per 1.48 gr of thyroid tissue. The study consisted of 11 males (%15.2) and 61 females (%84.8) with a mean age of 49.18 (range, 21-73). The clinicopathological characteristics of the cases with detected microcarcinomas after whole gland sampling ($n=29$, %40.2) are given in Table. The weight of cases with carcinomas was statistically higher compared to cases without cancer. The alike result was also observed regarding the age of patients. (Figure 2) There was also a statistically significant difference ($p=0.005$) between the sex of patients with and without carcinomas (9 of males had carcinoma out of 11 and 20 of females out of 61).

Clinicopathological Parameters of Cases with Microcarcinomas		Number of all cases (n = 72)	Percentage (%)
Presence of microcarcinomas		29	%37.9
Tumor types	Classical variant PMC	11	%37.8
	Follicular variant PMC	15	%51.6
	Follicular variant (oncoytic type) PMC	1	%3.5
	Oncocytic mixt follicular and classical variant PMC	1	%3.5
	Medullary microcarcinoma and follicular variant PMC	1	%3.5
Tumor localization	Right lobe	12	%41.3
	Left lobe	12	%41.3
	Isthmus	1	%3.4
	Bilateral	4	%14
Tumor size (mm) (mean ± standard deviation)		1.72 ± 0.89 (0.5-3.5)	
Encapsulation		9	%31
Capsular invasion (only for encapsulated tumors)		2	%22.2
Parenchyma invasion (only for non-encapsulated tumors)		2	%10
Lymphatic invasion		2	%6.8
Vascular invasion		0	%0
Lymph node metastasis		3	%10.3
Extrathyroidal extension / Surgical margin positivity		0/0	%0
Multifocality		10	%34.4

Figure 1 - 308

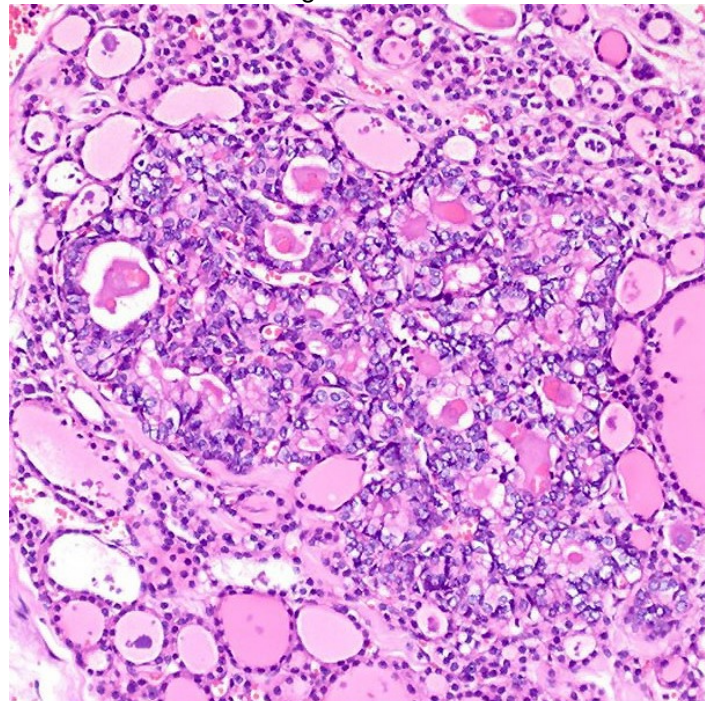
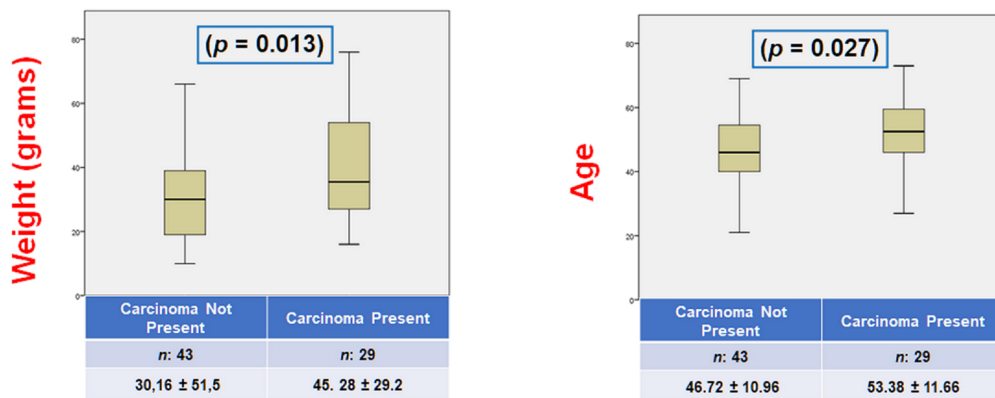


Figure 2 - 308



Conclusions: Despite all the care and attention shown, microcarcinoma foci may be hidden in the part of the thyroidectomy materials we throw away. Although extremely rare, the risk of future metastasis should be kept in mind in cases that are reported as benign. Pathologists and clinicians should be aware of these unwanted possibilities.

309 Solid Follicular Thyroid Nodules with Longitudinal Nuclear Grooves: Clinicopathologic, Immunohistochemical and Molecular Genetic Study of 18 Cases

David Suster¹, Alexander Mackinnon², Saul Suster³

¹Rutgers New Jersey Medical School/Rutgers University, Newark, NJ, ²The University of Alabama at Birmingham, Birmingham, AL, ³Medical College of Wisconsin, Milwaukee, WI

Disclosures: David Suster: None; Alexander Mackinnon: None

Background: Follicular nodules of the thyroid can be a source of diagnostic difficulties, particularly when they display nuclear features that are strongly associated with papillary thyroid carcinoma (PTC). However, as demonstrated by the recently introduced category of non-invasive follicular thyroid neoplasms with papillary-like nuclear features (NIFTP), not all lesions with nuclear features of PTC warrant a diagnosis of carcinoma.

Design: 18 cases of atypical solid follicular nodules with longitudinal nuclear grooves were collected and assessed for clinical and histopathologic characteristics. Cases that fit the criteria for NIFTP were excluded from this study. Immunohistochemistry was performed on each case using antibodies to HBME-1, CK19, galectin-3 and Ki-67. Next generation sequencing (NGS) was performed in 18 cases using a commercially available amplicon based 161 gene panel.

Results: The clinicopathologic and molecular features are summarized in table 1. Most of the cases were incidental findings in thyroids removed for other reasons; 83.3% of the cases were <1.0 cm. Histology showed relatively small, well circumscribed nodules that stood out from the surrounding thyroid parenchyma due to increased cellularity. The nodules in all cases were sharply demarcated from the surrounding tissue without evidence of invasion. The nodules were mostly composed of solid and compact microfollicular structures with collapsed lumens. Rare, well-developed small follicles with open lumens were seen. 5/18 (27%) cases showed cytoplasmic and membranous staining for HBME-1. All cases were negative for CK19, except for one case which was positive for CK19 but negative for HBME-1. Galectin-3 stains were negative. Ki-67 showed a low proliferative activity (<1% nuclear positivity) in all cases. RAS mutations were the most common molecular alteration occurring in 8/16 cases (50%). BRAF V600E was not identified in any case tested, however BRAF K601E was present in 4/16 (25%) of cases. Variants in HNF1A, ATM, and MET were not considered clinically significant. Clinical follow-up ranging from 18-72 months (median= 43.7) did not disclose any evidence of recurrence or metastases.

TABLE 1: Clinical and pathologic features of solid follicular thyroid nodules with longitudinal nuclear grooves.

Case	Sex/Age	Clinical Presentation and Procedure	Size/location	Pathologic findings	IHC	Molecular
1	F/52	Rt. Lobectomy for 3.5 cm. nodule	0.4 cm, right lobe	Nodular hyperplasia with chronic lymphocytic thyroiditis. The 3.5 cm nodule was a "dominant" hyperplastic nodule. Incidental 0.4 cm, solid nodule with longitudinal nuclear grooves.	CK19/HBME (-)	NMA
2	F/52	Total thyroidectomy for multinodular goiter	0.4 cm, left lobe	Nodular hyperplasia. Incidental 0.4 cm, solid nodule with longitudinal nuclear grooves.	CK19/ (-) HBME Focal + (2% of cells)	NRAS – p.Q61R HNF1A – p.R114H
3	F/36	Total thyroidectomy for multinodular goiter	0.6 cm, right lobe	Nodular hyperplasia. Incidental 0.6 cm, solid nodule with longitudinal nuclear grooves.	CK19/HBME (-)	NRAS – p.Q61R
4	F/88	Rt. Lobectomy for "suspicious" 2.5 cm nodule; parathyroidectomy for 1ry HPT	1.5 cm, right lobe	Nodular hyperplasia with "dominant" 2.5 cm hyperplastic nodule and incidental micro-PTC 1 mm diameter. 1.5 cm, solid nodule with longitudinal nuclear grooves.	CK19/HBME (-)	NMA
5	F/57	Total thyroidectomy for multinodular goiter	0.8 cm, left lobe	Nodular hyperplasia. Incidental 0.8 cm, solid nodule with longitudinal nuclear grooves.	HMBE+ CK19 (-)	Not done
6	F/46	Total thyroidectomy for multinodular goiter	0.2 cm, right lobe	Nodular hyperplasia. Incidental 0.2 cm, solid nodule with longitudinal nuclear grooves.	HBME+ CK19 (-)	NMA
7	F/50	Sickle cell disease and multinodular goiter, total thyroidectomy	0.6 cm., isthmus	Nodular hyperplasia. Incidental 0.6 cm, solid nodule with longitudinal nuclear grooves.	CK19/HBME (-)	NRAS – p.Q61R
8	F/45	Rt. lobectomy for 1.2 cm. solitary nodule.	0.7 cm, right lobe	Nodular hyperplasia with 1.2 cm. adenomatoid nodule. Incidental 0.7 cm, solid nodule with longitudinal nuclear grooves.	HBME Focal + CK19 (-)	BRAF – p.K601E
9	F/60	Total thyroidectomy for multinodular goiter	0.5 cm, left lobe	Nodular hyperplasia. Incidental 0.5 cm, solid nodule with longitudinal nuclear grooves.	HBME1 Focal + CK19 (-)	HRAS – p.Q61R
10	F/64	Nodular goiter with FNA dx of atypia; total thyroidectomy	0.6 cm, right lobe	Nodular hyperplasia. Incidental 0.6 cm, solid nodule with longitudinal nuclear grooves.	HBME1 (-) CK19 +	BRAF – p.K601E ATM – p.R3371I
11	F/53	Right lobectomy and isthmusectomy for palpable nodule, "suspicious for PTC" on FNA	1.2 cm, right lobe	Nodular hyperplasia. 1.2 cm, solid nodule with longitudinal nuclear grooves.	HBME1 focal + CK19 (-)	NRAS – p.Q61R
12	F/45	Total thyroidectomy for multinodular goiter	0.6 cm, right lobe	Nodular hyperplasia. Incidental 0.6 cm, solid nodule with longitudinal nuclear grooves.	CK19/HBME (-)	NRAS – p.Q61R

13	F/58	Total thyroidectomy for 2.5 cm "suspicious" nodule on FNA in left lobe	0.6 cm, right lobe	Nodular hyperplasia with incidental papillary microcarcinomas., multifocal, bilateral. 2.5 cm. "dominant" adenomatoid nodule, left lobe. Incidental 0.6cm, solid nodule with longitudinal nuclear grooves.	CK19/HBME (-)	NMA
14	F/61	Total thyroidectomy for multinodular goiter and Hashimoto	0.6 cm, right lobe	Nodular hyperplasia with incidental focus of micropapillary carcinoma 0.2 cm. (contralateral lobe) Incidental 0.6 cm, solid nodule with longitudinal nuclear grooves.	HBME + CK19 (-)	BRAF – p.K601E
15	M/72	Total thyroidectomy for multinodular goiter	0.7 cm, left lobe	Nodular hyperplasia with multiple incidental foci of micropapillary carcinoma, 0.3-0.5 cm., bilateral. Incidental 0.7 cm, solid nodule with longitudinal nuclear grooves.	HBME1 + (also in adjacent adenomatoid nodules) CK19 (-)	HRAS – p.Q61K MET – p.T1010I
16	M/47	Total thyroidectomy for multinodular goiter	1.2 cm, right lobe	Nodular hyperplasia. Incidental 1.2 cm, solid nodule with longitudinal nuclear grooves.	HBME1 + CK19 (-)	NRAS – p.Q61R
17	F/54	FNA positive for PTC Total thyroidectomy for multinodular goiter and PTC	0.4 cm, right lobe	Nodular hyperplasia with multifocal micropapillary carcinomas, bilateral, and 2.5 cm. PTC in left lobe. Incidental 0.4 cm solid nodule with longitudinal nuclear grooves.	CK19/HBME (-)	BRAF – p.K601E
18	F/39	Lt. lobectomy for suspicious nodule on FNA	0.7 cm, left lobe	0.7 cm solid nodule with longitudinal nuclear grooves.	HBME+ CK19 (-)	Not done

*NMA = No molecular abnormalities detected; PTC= papillary thyroid carcinoma; FNA= fine needle aspiration.

Conclusions: 18 patients who presented with small, well-circumscribed, largely unencapsulated and noninvasive, predominantly solid follicular thyroid nodules containing longitudinal nuclear grooves were examined. Most cases in our study were negative for immunohistochemical or molecular markers that have been traditionally associated with PTC. *RAS* and *BRAF* K601E mutations were present in a significant proportion of these tumors. The results raise the question of whether these lesions represent novel pre-malignant neoplastic follicular lesions or a perhaps a "solid" variant of NIFTP, however it is unlikely they represent any type of PTC despite the presence of nuclear grooves.

310 Clinicopathologic and Molecular Characteristics of Resected Primary Poorly Differentiated Thyroid Carcinoma (PDTC): A Single-Institution Retrospective Study of 364 Cases

Bin Xu¹, Snjezana Dogan¹, Nora Katabi¹, Maelle Saliba¹, Anjanie Khimraj¹, James Fagin¹, Ronald Ghossein¹

¹Memorial Sloan Kettering Cancer Center, New York, NY

Disclosures: Bin Xu: None; Snjezana Dogan: None; Nora Katabi: None; Maelle Saliba: None; Anjanie Khimraj: None; James Fagin: *Grant or Research Support, Eisai; Advisory Board Member, Loxo Oncology/Eli Lilly*; Ronald Ghossein: None

Background: There is a need to investigate the clinical, pathologic, and molecular features of PDTC.

Design: 364 patients with resected primary PDTC defined using MSKCC criteria (i.e. mitotic index 5/10 HPFs and/or tumor necrosis) were included. Next generation sequencing using MSK-IMPACT platform was performed in 166 patients.

Results: The median age of diagnosis was 58 (range 5-90) and female to male ratio was 1.3:1. 200 patients (54.9%) additionally fulfilled the Turin definition; whereas the remaining 164 only met the MSKCC definition and might be regarded as high grade papillary carcinoma (n=155) or follicular carcinoma (n=9). Vascular invasion (VI), AJCC pT3/T4, nodal metastasis, and positive margin were common findings, being seen in 69.7%, 56.1%, 32.4%, and 35.1% respectively. Follow-up (FU) was available in 346 patients with a median FU period of 5.3 years. The 3-year, 5-year, 10-year, and 20-year disease specific survival (DSS) was 89%, 76%, 60% and 35% respectively. Distant metastasis (DM) occurred in 216 (62%) patients, including 84 with DM at initial presentation and 11 developed DM more than 10 years after the thyroid resection. Multivariate analysis (**Figure**) showed that independent prognostic factors were age, sex, tumor size, and encapsulation for DSS; age, sex, and VI for DM free survival (DMFS); and necrosis, margin and nodal status for locoregional recurrence free survival. Turin-PDTC had similar DSS but higher frequency of DM compared with non-Turin PDTC. 17 patients had encapsulated noninvasive PDTC. Among the 16 cases with FU, 3 developed DM and 1 died of his disease. The frequency of *BRAF*, *RAS*, *TERT*, and *TP53* alterations was 28%, 40%, 55% and 11% respectively. Compared with *BRAF* V600E-mutated PDTC, *RAS*-mutants were associated with higher frequency of VI, DM and Turin-PDTC, and lower rate of nodal metastasis. *TERT* promoter mutation was an independent prognostic factor for DMFS when adjusted for AJCC stage, age and sex. Co-existing *TERT* mutation significantly increased the risk of DM in *BRAF* V600E-mutated PDTCs but not in *RAS*-mutants. Molecular alterations did not impact DSS.

Figure 1 - 310

Table. Multivariate survival analysis using Cox proportional model. Factors significant on univariate survival analysis were selected for multivariate analysis. Red p values: significant p values.		
	P value	Hazard ratio (95% confidence interval)
DSS		
Age	<0.001	1.900 (1.419-2.545)
Sex	.243	1.313 (0.831-2.075)
Tumor necrosis	.069	1.383 (0.975-1.962)
Tumor size	.012	1.866 (1.144-3.040)
Encapsulation	.037	0.501 (0.261-0.960)
Vascular invasion	.369	0.761 (0.420-1.380)
Gross ETE	.195	1.575 (0.792-3.133)
Microscopic ETE	.345	1.183 (0.835-1.677)
AJCC 8th pT	.485	0.843 (0.522-1.361)
N stage	.160	1.416 (0.872-2.298)
Margin status	.582	1.142 (0.712-1.831)
DMFS		
Age	<0.001	1.514 (1.266-1.812)
Sex	.016	1.473 (1.075-2.020)
Tumor necrosis	.186	1.173 (0.926-1.485)
Tumor size	.144	1.345 (0.904-1.999)
Encapsulation	.120	0.718 (0.473-1.090)
Vascular invasion	.030	1.613 (1.048-2.484)
Turin criteria	.914	1.022 (0.687-1.519)
PTC nuclei	.990	0.998 (0.701-1.421)
FTC/convoluted nuclei	.523	1.137 (0.766-1.688)
Gross ETE	.949	0.983 (0.580-1.666)
Microscopic ETE	.076	1.261 (0.976-1.628)
AJCC 8th pT	.352	0.841 (0.585-1.210)
Margin status	.307	1.212 (0.839-1.750)
Locoregional recurrence free survival		
Sex	.567	1.132 (0.741-1.730)
Tumor necrosis	.005	1.653 (1.160-2.356)
Tumor size (cm)	.091	1.522 (0.935-2.478)
Encapsulation	.172	0.650 (0.351-1.207)
Microscopic ETE	.645	0.917 (0.635-1.324)
Gross ETE	.680	0.860 (0.421-1.759)
AJCC 8th pT	.672	1.105 (0.697-1.751)
Margin status	.024	1.759 (1.059-2.867)
N stage	.001	2.223 (1.369-3.609)

Conclusions: 1) PDTC incurs poor long-term survival and high risk of DM. 2) Independent prognostic factors in PDTC are age, sex, tumor size, encapsulation, VI, necrosis, margin and nodal status. 3) *TERT* promoter mutation is an independent prognostic factor for DMFS in PDTC. 4) *RAS*-mutants are associated with higher frequency of VI and DM. 5) Noninvasive encapsulated PDTC can have DM and mortality.